How to cite: *Angew. Chem. Int. Ed.* **2020**, *59*, 21945–21948
International Edition: doi.org/10.1002/anie.202009230
German Edition: doi.org/10.1002/ange.202009230

Methanol-to-Olefins | Hot Paper

Control of Surface Barriers in Mass Transfer to Modulate Methanol-to-Olefins Reaction over SAPO-34 Zeolites

Shichao Peng, Mingbin Gao, Hua Li, Miao Yang, Mao Ye,* and Zhongmin Liu*

Abstract: *Mass transfer of guest molecules has a significant impact on the applications of nanoporous crystalline materials and particularly shape-selective catalysis over zeolites. Control of mass transfer to alter reaction over zeolites, however, remains an open challenge. Recent studies show that, in addition to intracrystalline diffusion, surface barriers represent another transport mechanism that may dominate the overall mass transport rate in zeolites. We demonstrate that the methanol-to-olefins (MTO) reaction can be modulated by regulating surface permeability in SAPO-34 zeolites with improved chemical liquid deposition and acid etching. Our results explicitly show that the reduction of surface barriers can prolong catalyst lifetime and promote light olefins selectivity, which opens a potential avenue for improving reaction performance by controlling the mass transport of guest molecules in zeolite catalysis.*

Mass transfer of guest molecules in nanoporous crystalline materials is of fundamental significance in processes spanning heterogenous catalysis and gas separation.[1] One of particularly notable applications is zeolite catalysts widely utilized for producing liquid fuel and chemicals, in favor of the unique shape selectivity.[2] Routinely limitation of mass transfer, especially molecular diffusion, which is related to topological structures of zeolites and steric dimension of molecules, is considered governing shape-selective catalysis. The mechanism underlying molecular diffusion in zeolites, however, is quite involved and not yet fully understood.

It was recently found that, despite the well-acknowledged intracrystalline diffusion that is intrinsic to molecular properties and material structures, surface barriers represent another important transport mechanism.[3] The origins of surface barriers, though not fully understood, are closely related to the non-ideality of zeolite crystals which can be the consequences of, among others, surface modification, defects formation, and pores decoration.[4] As revealed by interference microscopy (IFM) and infrared microscopy (IRM),[4b,5] surface barriers may dominate the overall mass transport rate in zeolite catalysts. Despite the importance of surface resistance in mass transfer over zeolite crystals being qualitatively identified, controlling the performance of catalytic reaction by directed modulation of surface barriers remains an open challenge.

Methanol-to-olefins (MTO), first commercialized in 2010, has gained considerable interests for effectively producing ethylene and propylene from alternative resources such as natural gas, coal, and biomass.[6] SAPO-34 zeolites have been accepted well suitable for MTO owing to the special chabazite (CHA)-type structure, in which heavy aromatic species are readily generated and accumulated within cavities during olefins formation. This can result in the pronounced mass transport limitation for the large molecules and thus the enhanced light olefins selectivity.[7] It is shown by IFM that the dominating transport mechanism of methanol in SAPO-34 zeolites is surface barriers.[4b] Based on the distribution of coke species (i.e. heavy aromatics) observed by confocal fluorescence microscopy (CFM), the researchers further speculated that surface barriers may have significant impact on MTO reaction.[8] This provides important and practical implications on the possibility of altering MTO reaction via regulating the mass transport. In this work, for the first time, we demonstrate the modulation of MTO reaction over SAPO-34 zeolites by controlling surface permeability of guest molecules.

The external surface of zeolite crystals can be decorated by post-synthesis treatments,[9] including chemical liquid/vapor deposition (CLD/CVD) and HF etching. However, modifying zeolite surfaces by these conventional methods would cause the suppression of acid density[10] and damage of internal structure of crystals,[11] unavoidably changing intracrystalline diffusivities of guest molecules. To achieve the modulation of surface barriers, a prerequisite is that the modification is only made for external surface of crystals while the change of interiors is negligible. In doing so, SAPO-34 zeolite samples were first synthesized hydrothermally[12] and denoted as SAPO-34-B. Then part of SAPO-34-B samples were decorated by CLD of tetraethoxysilane (TEOS), denoted as SAPO-34-L. In the CLD treatment, although the SiO_2 on the outer surface may increase the surface sticking probability, multiple deposits likely cause pore blockage.[2b] As a consequence, it is more difficult for molecules to enter the crystals, resulting in the pronounced surface barriers or low surface permeability in SAPO-34-L. As the large molecules of TEOS could hardly pass the nanopores, the decoration was expected to occur on the external surface of SAPO-34-L. Parts of SAPO-34-B samples were treated by etching with acetic acidic solution, removing

[*] S. Peng, M. Gao, Dr. H. Li, Dr. M. Yang, Prof. Dr. M. Ye, Prof. Dr. Z. Liu
National Engineering Laboratory for Methanol-to-Olefins, Dalian National Laboratory for Clean Energy, Dalian Institute of Chemical Physics, Chinese Academy of Sciences
Dalian 116023 (P. R. China)
E-mail: lihua@dicp.ac.cn
maoye@dicp.ac.cn
S. Peng, M. Gao
University of Chinese Academy of Sciences
Beijing 100049 (P. R. China)
Supporting information and the ORCID identification number(s) for the author(s) of this article can be found under: https://doi.org/10.1002/anie.202009230.

the structural defects and opening the orifices.[3b] These samples would have reduced surface barriers, denoted as SAPO-34-H. As organic template could effectively prevent acetic acid from entering the interior, a minor change of internal structures of SAPO-34-H is also expected. Furthermore, a decrease of acid strength for etching was achieved to avoid the destruction of crystals and assure the stability of samples. The details of synthesis and modifications are described in Supporting Information.

The changes of interior structure and acid properties of SAPO-34 zeolites after modifications were carefully examined. The XRD patterns of all three SAPO-34 samples are shown in Figure 1 a, which manifest typical characteristic diffraction peaks of the CHA topology, showing the stability of zeolites to the surface modifications. Table S1 in the Supporting Information shows the relative crystallinity calculated based on the characteristic peaks at $2\theta = 9.4$, 12.8 and 20.5°, and indicates that the relative crystallinity is invariant for three samples. The SEM images of three samples are depicted in the Supporting Information, Figure S1, showing a similar morphology of cubic crystals with an average size of 2 μm and no clear morphological changes after surface modifications. The Si/Al molar ratios (Table S1) suggest that the compositions of crystals are essentially the same for three samples. Figure 1 b shows the N_2 adsorption-desorption isotherms, and the corresponding properties are also reported in Table S1. The treated zeolites exhibit similar micropore surface area and volume with the SAPO-34-B and little mesopore volume can be detected, which suggests that there are no obvious changes in pore structure after treatments. From the NH_3-TPD curves (Figure 1 c), two separated desorption peaks exist around 187 and 421 °C, corresponding to weak and strong acid sites in the samples, and no significant changes have been observed in the strength of surface acid sites. Besides, the acid densities of three SAPO-34 samples are similar (Table S1). In diffuse reflectance infrared Fourier transform spectroscopy (DRIFTS) as shown in Figure 1 d, the absorption bands at around 3616 and 3594 cm^{-1} are assigned to the vibrations associated with bridging hydroxyl (Si-OH-Al) groups,[13] which refer to Brønsted acid sites, that is, the active sites for MTO reaction. As can be seen, DRIFTS profiles are nearly uniform, indicating that Brønsted acid sites were almost unaffected by the decoration of surfaces. Thus it can be summarized that, based on the structure, texture and acidic property of the three SAPO-34 samples shown in Figure 1 and Table S1, all three SAPO-34 samples have nearly the same intracrystalline characteristics regardless of the treatments.

The surface barriers and intracrystalline diffusion of guest molecules were quantified through uptake rate measurements. The dual resistance model (DRM) has been proposed to account for the combined effect of surface barriers and intracrystalline diffusion in uptake rate profile:[14]

$$\frac{m_t}{m_\infty} = 1 - \sum_{n=1}^{\infty} \frac{2L^2 \exp\left(-\frac{\beta_n^2 Dt}{l^2}\right)}{(\beta_n^2 + L^2 + L)\,\beta_n^2}; \quad \beta_n \tan\beta_n = L = \frac{\alpha l}{D} \tag{1}$$

where m_t/m_∞ is the normalized loading, t the uptake time, D the intracrystalline diffusivity, α the surface permeability, and l the equivalent radius. Nevertheless, DRM requires in prior information of D to derive α or vice versa. Recently, Gao et al[15] proposed to estimate α from the initial uptake rate

$$\frac{m_t}{m_\infty}\Big|^{\sqrt{t}\to 0} \cong \frac{\alpha}{l}(\sqrt{t})^2 \tag{2}$$

and D from the fitting of uptake curves with DRM. The SAPO-34 zeolite crystals are approximately treated as cubes with the equivalent radius calculated by $l = b/4.06$, where b represents the length of crystal.

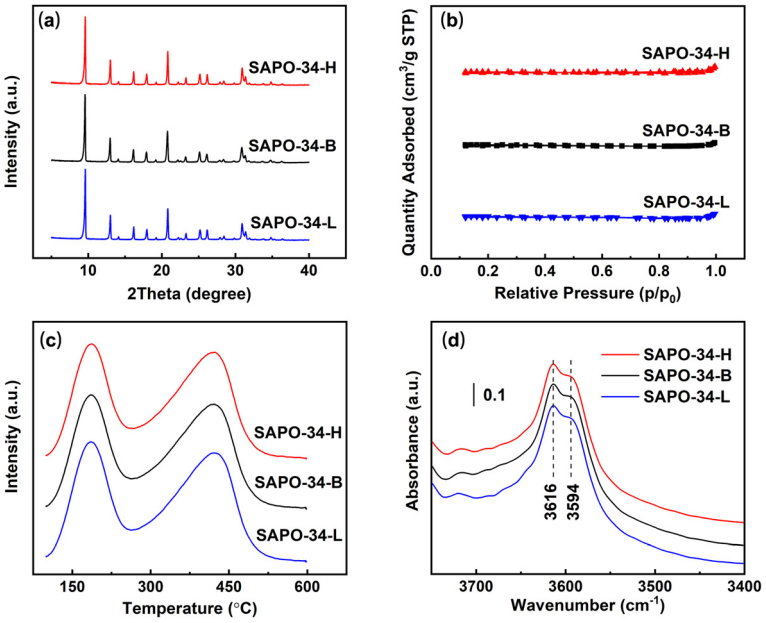

Figure 1. a) XRD patterns, b) nitrogen adsorption–desorption isotherms, c) NH_3-TPD profiles, and d) DRIFT spectra of three SAPO-34 samples.

It should be stressed α and D varies with guest molecules of interest. However, MTO reaction is very complicated and many intermediates and products would be formed. The surface barriers are dependent upon the guest molecules in terms of size, structure, and polarity. In MTO the ethene and propene are targeted products. It is shown that the kinetic diameter of propene is comparable to the size of nanopores of SAPO-34 zeolites, and the limitation of diffusion of molecules larger than propene leads to the high light olefins selectivity.[16] To minimize the influence of adsorption and reaction, propane, rather than propene, was used as the model molecule in deriving α and D. The adsorption curve of propane at 40 °C was measured by intelligent gravimetric analyzer (IGA), which was further used to derive α and D for three SAPO-34 samples. Figure 2 show α and D of propane fitted with Equations (1) and (2). For propane, similar D is observed for all three samples, which is in accordance with the uniform structural, textural and acid properties shown in

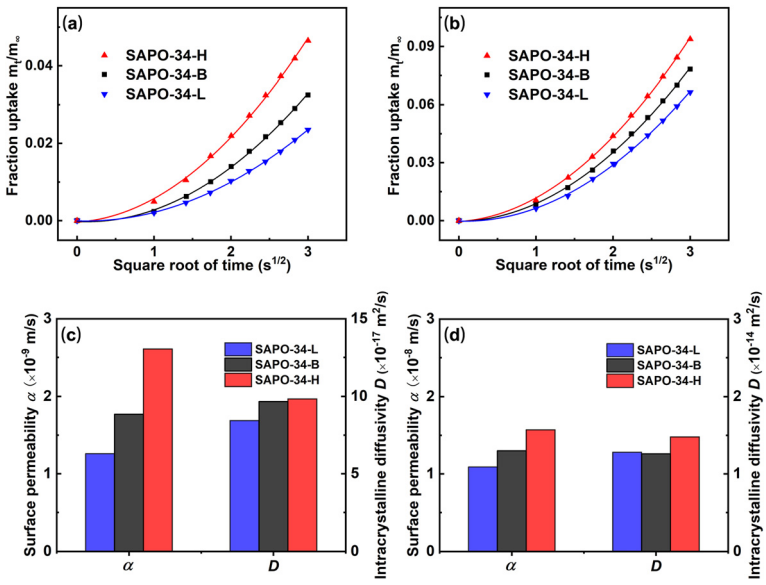

Figure 2. a) Initial uptake rates of propane at 40 °C and of b) methanol at 20 °C in three SAPO-34 samples. The scatters represent the experimental data while solid lines are fitting results determined with Equation (2). The correlation coefficient R^2 of all fitting is greater than 0.999. c,d) Surface permeability and intracrystalline diffusivity of propane (c) and methanol (d) derived from the uptake rates (Figure S2) following the method of Gao et al.[15]

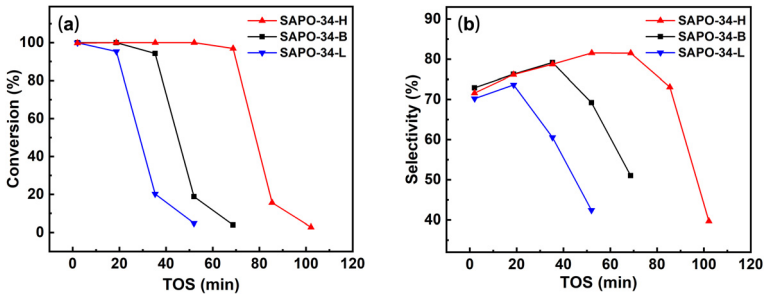

Figure 3. a) Methanol conversion and b) light olefins (ethene, propene) selectivity as a function of time on stream (TOS) in MTO reaction over SAPO-34 samples. Reaction condition: 450 °C, methanol WHSV = 5.0 h^{-1}.

Figure 1. An apparent increase in α is observed for three samples in the order of SAPO-34-L, SAPO-34-B and SAPO-34-H. For comparison, the adsorption curve of methanol was also measured by IGA at 20 °C. Similar trends of D and α can also be observed for methanol for three samples.

As effective diffusivity has been frequently applied to understand molecular transport, we also calculated the effective diffusivity.[4b] It is found that, although the variation of effective diffusivity is in accordance with our findings for surface permeability, the mechanism of mass transport cannot be directly inferred. A detailed discussion is including in Supporting Information.

The SAPO-34 samples were evaluated by performing MTO reaction at 450 °C under atmospheric pressure with a weight hourly space-velocity (WHSV) of 5.0 h^{-1}. Figures 3 a,b illustrate the methanol conversion and light olefins selectivity. The catalyst lifetime is defined as the time with methanol conversion above 95 %. It is shown that the catalyst lifetime for SAPO-34-B is 35 min, which, after modification, is extended to 69 min for SAPO-34-H and shortened to 19 min for SAPO-34-L. Considering that the interior structures of crystals were almost unchanged as revealed above, the variation of catalyst lifetime could be mainly related to surface barriers of guest molecules, that is, SAPO-34 zeolites would have an extended lifetime in MTO reaction with the increase of surface permeability. Figure 4 further shows the surface permeabilities of propane and methanol with regard to catalyst lifetime. As can be seen, catalyst lifetime depicts a linearly increase with surface permeability of guest molecules. It is not clear at present whether such a linear relation is intrinsic or not, which nevertheless deserves further study. As for the light olefins selectivity, it is shown in Figure 3 b that SAPO-34-H which has reduced surface barriers exhibits higher peak selectivity of 81.6 %, while SAPO-34-L which has enhanced surface barriers shows a low peak selectivity of 73.6 %. Note that peak light olefins selectivity for SAPO-34-B is 79.2 %.

It has been previously shown that surface barriers would symmetrically affect guest molecules in moving in and out of the zeolite crystals.[17] The increase of surface barriers would limit the corresponding guest molecules diffuse outward the crystals during MTO reaction and enhance further transformation of light olefins to heavy aromatics in the cavities, which lowers the light olefins yield and weakens the resistance to inactivation. In this sense, a shorter catalyst lifetime and lower light olefins selectivity is expected. Therefore, it is possible to modulate catalyst lifetime and light olefins selectivity in MTO reaction by controlling the surface barriers in SAPO-34 zeolites.

In conclusion, for the first time we demonstrate that the control of surface barriers in SAPO-34 zeolites can be applied to modulate catalyst lifetime and light olefins selectivity in the MTO reaction. Through CLD and acid etching, we can modify the surface properties while maintaining the morphology, internal structure and acid properties of SAPO-34 zeolites, which makes it possible to regulate surface permeability without changing the intracrystalline diffusivity of guest molecules. Essentially, decreasing surface barriers should extend the catalyst lifetime and result in improved light olefins selectivity. Explicit evidence is provided for the correlation between surface barriers and catalytic performance. As such, this work provides a strategy toward improving reaction performance by controlling mass transport of guest molecules in zeolite catalysis.

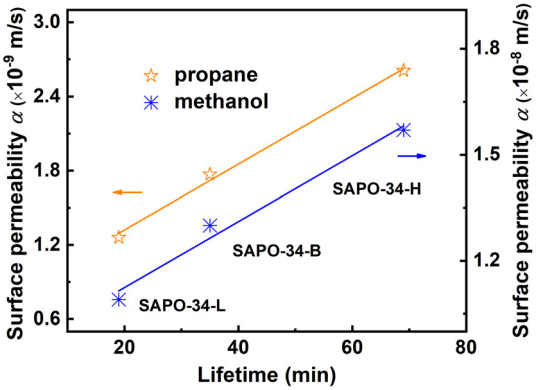

Figure 4. The surface permeability of propane and methanol with regard to the lifetime of SAPO-34 zeolites. The scatters represent the experimental data while solid lines are linearly fitted results.

Acknowledgements

This work is supported by the National Natural Science Foundation of China (Grant No.91834302).

Conflict of interest

The authors declare no conflict of interest.

Keywords: guest molecules · mass transfer · SAPO-34 · surface barriers · zeolite catalysis

[1] a) G. T. Whiting, N. Nikolopoulos, I. Nikolopoulos, A. D. Chowdhury, B. M. Weckhuysen, *Nat. Chem.* **2019**, *11*, 23 – 31; b) Z. Guo, X. Li, S. Hu, G. Ye, X. Zhou, M. O. Coppens, *Angew. Chem. Int. Ed.* **2020**, *59*, 1548 – 1551; *Angew. Chem.* **2020**, *132*, 1564 – 1567; c) Y. Wu, S. Zeng, D. Yuan, J. Xing, H. Liu, S. Xu, Y. Wei, Y. Xu, Z. Liu, *Angew. Chem. Int. Ed.* **2020**, *59*, 6765 – 6768; *Angew. Chem.* **2020**, *132*, 6831 – 6834; d) K. Li, D. H. Olson, J. Seidel, T. J. Emge, H. Gong, H. Zeng, J. Li, *J. Am. Chem. Soc.* **2009**, *131*, 10368 – 10369; e) G. Ye, Y. Sun, Z. Guo, K. Zhu, H. Liu, X. Zhou, M.-O. Coppens, *J. Catal.* **2018**, *360*, 152 – 159; f) M. Gao, H. Li, W. Liu, Z. Xu, S. Peng, M. Yang, M. Ye, Z. Liu, *Nat. Commun.* **2020**, *11*, 3641.

[2] a) U. Olsbye, S. Svelle, M. Bjorgen, P. Beato, T. V. Janssens, F. Joensen, S. Bordiga, K. P. Lillerud, *Angew. Chem. Int. Ed.* **2012**, *51*, 5810 – 5831; *Angew. Chem.* **2012**, *124*, 5910 – 5933; b) S. Zheng, H. R. Heydenrych, H. P. Roger, A. Jentys, J. A. Lercher, *Top. Catal.* **2003**, *22*, 101 – 106; c) S. Zheng, A. Jentys, J. Lercher, *J. Catal.* **2006**, *241*, 304 – 311.

[3] a) L. Heinke, J. Karger, *Phys. Rev. Lett.* **2011**, *106*, 074501; b) F. Hibbe, C. Chmelik, L. Heinke, S. Pramanik, J. Li, D. M. Ruthven, D. Tzoulaki, J. Karger, *J. Am. Chem. Soc.* **2011**, *133*, 2804 – 2807; c) S. M. Rao, E. Saraçi, R. Gläser, M.-O. Coppens, *Chem. Eng. J.* **2017**, *329*, 45 – 55.

[4] a) W. L. Duncan, K. P. Moller, *Adsorp. J. Int. Adsorp. Soc.* **2005**, *11*, 259 – 273; b) J. C. Saint Remi, A. Lauerer, C. Chmelik, I. Vandendael, H. Terryn, G. V. Baron, J. F. Denayer, J. Karger, *Nat. Mater.* **2016**, *15*, 401 – 406.

[5] a) J. Kärger, T. Binder, C. Chmelik, F. Hibbe, H. Krautscheid, R. Krishna, J. Weitkamp, *Nat. Mater.* **2014**, *13*, 333 – 343; b) L. Zhang, C. Chmelik, A. N. van Laak, J. Karger, P. E. de Jongh, K. P. de Jong, *Chem. Commun.* **2009**, 6424 – 6426; c) C. Chmelik, J. Karger, *Chem. Soc. Rev.* **2010**, *39*, 4864 – 4884.

[6] a) M. Stöcker, *Microporous Mesoporous Mater.* **1999**, *29*, 3 – 48; b) M. Ye, H. Li, Y. Zhao, T. Zhang, Z. Liu, *Adv. Chem. Eng.* **2015**, *47*, 279 – 335.

[7] a) S. Gao, S. Xu, Y. Wei, Q. Qiao, Z. Xu, X. Wu, M. Zhang, Y. He, S. Xu, Z. Liu, *J. Catal.* **2018**, *367*, 306 – 314; b) W. Dai, G. Wu, L. Li, N. Guan, M. Hunger, *ACS Catal.* **2013**, *3*, 588 – 596; c) P. Tian, Y. Wei, M. Ye, Z. Liu, *ACS Catal.* **2015**, *5*, 1922 – 1938.

[8] a) L. Karwacki, E. Stavitski, M. H. Kox, J. Kornatowski, B. M. Weckhuysen, *Angew. Chem. Int. Ed.* **2007**, *46*, 7228 – 7231; *Angew. Chem.* **2007**, *119*, 7366 – 7369; b) D. Mores, E. Stavitski, M. H. Kox, J. Kornatowski, U. Olsbye, B. M. Weckhuysen, *Chem. Eur. J.* **2008**, *14*, 11320 – 11327; c) Q. Qian, J. Ruiz-Martinez, M. Mokhtar, A. M. Asiri, S. A. Al-Thabaiti, S. N. Basahel, H. E. van der Bij, J. Kornatowski, B. M. Weckhuysen, *Chem. Eur. J.* **2013**, *19*, 11204 – 11215.

[9] a) X. Hou, Y. Qiu, X. Zhang, G. Liu, *RSC Adv.* **2016**, *6*, 54580 – 54588; b) J. Wloch, *Microporous Mesoporous Mater.* **2003**, *62*, 81 – 86; c) S. J. Reitmeier, O. C. Gobin, A. Jentys, J. A. Lercher, *Angew. Chem. Int. Ed.* **2009**, *48*, 533 – 538; *Angew. Chem.* **2009**, *121*, 541 – 546; d) O. C. Gobin, S. J. Reitmeier, A. Jentys, J. A. Lercher, *J. Phys. Chem. C* **2011**, *115*, 1171 – 1179.

[10] S. R. Zheng, H. R. Heydenrych, A. Jentys, J. A. Lercher, *J. Phys. Chem. B* **2002**, *106*, 9552 – 9558.

[11] G. Ye, Z. Guo, Y. Sun, K. Zhu, H. Liu, X. Zhou, M.-O. Coppens, *Chem. Ing. Tech.* **2017**, *89*, 1333 – 1342.

[12] G. Liu, P. Tian, J. Li, D. Zhang, F. Zhou, Z. Liu, *Microporous Mesoporous Mater.* **2008**, *111*, 143 – 149.

[13] S. Bordiga, L. Regli, D. Cocina, C. Lamberti, M. Bjørgen, K. P. Lillerud, *J. Phys. Chem. B* **2005**, *109*, 2779 – 2784.

[14] J. Kärger, D. M. Ruthven, *New J. Chem.* **2016**, *40*, 4027 – 4048.

[15] M. Gao, H. Li, M. Yang, S. Gao, P. Wu, P. Tian, S. Xu, M. Ye, Z. Liu, *Commun. Chem.* **2019**, *2*, 43.

[16] a) H. Oikawa, Y. Shibata, K. Inazu, Y. Iwase, K. Murai, S. Hyodo, G. Kobayashi, T. Baba, *Appl. Catal. A* **2006**, *312*, 181 – 185; b) P. Cnudde, R. Demuynck, S. Vandenbrande, M. Waroquier, G. Sastre, V. Van Speybroeck, *J. Am. Chem. Soc.* **2020**, *142*, 6007 – 6017.

[17] a) G. Sastre, J. Kärger, D. M. Ruthven, *J. Phys. Chem. C* **2019**, *123*, 19596 – 19601; b) D. M. Ruthven, *J. Phys. Chem. C* **2015**, *119*, 29201 – 29202.

Manuscript received: July 3, 2020
Revised manuscript received: August 24, 2020
Accepted manuscript online: September 3, 2020
Version of record online: October 7, 2020

